## 10 SCIENTIFIC HIGHLIGHT OF THE MONTH

**April 1999; http://www.dl.ac.uk/TCSC/HCM/PSIK/highlights.html**

---

# Nanotubes: Mechanical and Spectroscopic Properties

E. Hernández[1] and Angel Rubio[2]
[1]*School of Chemistry, Physics and Environmental Science, University of Sussex, Brighton BN1 9QJ, England UK*
*E-mail address: ehe@boltzmann.fam.cie.uva.es*
[2]*Departamento de Física Teórica, Universidad de Valladolid, E-47011 Valladolid, Spain.*
*E-mail address: arubio@mileto.fam.cie.uva.es*

**Abstract**

Fullerenes, and especially nanotubes, have caused a revolution in chemical physics and materials science in recent years. The unusual structure of these materials results in novel properties that make them interesting not only from a purely scientific perspective; given that these properties are of technological relevance, fullerenes and nanotubes could prove to have wide applicability in nano-technology. In this contribution we provide an overview of this rapidly growing field, focusing mostly on the role played by theoretical electronic structure methods (both semi-empirical and first-principles) in two important aspects of nanotube research: the mechanical and electronic properties of nanotubes, which are of key relevance to practical applications and to our present understanding of low dimensional structures.

## 10.1 Introduction

The discovery of $C_{60}$ [1], the finding of a way to produce it in large quantities [2] and the subsequent discovery of nanotubes [3], are findings that have opened a completely new field in the science of carbon related materials. Since these discoveries were made, fullerene and nanotube research has become a dynamic and rapidly growing field; ample proof of this fact can be found in a recent survey of publications related to this topic [4]. This survey shows that publications in the field can now be counted in thousands (their number was approaching 15000 at the time the survey was carried out), but perhaps more importantly, the rate of growth of the number of publications relating to fullerenes and nanotubes is increasing every year. This is a clear indication of the fact that more and more research groups are being attracted to this field of research. There are two main reasons for this. On the one hand, fullerenes and nanotubes are novel structures, displaying many interesting properties. The characterisation and understanding of these properties is one aim of research in the field. On the other hand, it is precisely these new properties that make fullerenes, and especially nanotubes, potentially useful in many applications related to nanotechnology. This potential for application is another attractive feature of this field of research.

Nanotubes appear as perfectly graphitized ($sp^2$ basic structural units), in either single-wall or multi-wall form, with carbon atoms arranged on each shell with various degrees of helicity and capped with pentagons just like the fullerene molecules. Multi-wall nanotubes (MWNT's) are generally in the range of 1-25 nanometers in diameter, while single-wall nanotubes (SWNT's) have diameters in the range 1-2 nm. Both SW and MW nanotubes are usually many microns long and hence they can fit well as components in submicrometer-scale devices and nanocomposite structures that are very important in emerging technologies. Furthermore, SWNT's are mostly arranged in ropes with a close packing stacking [5, 6] forming self-assembled cables that could be the ultimate light-weight high-strength flexible fiber. Recently much progress has been made in the production and purification of SW and MW carbon nanotubes in high yield, as well as in electronic, transport, optical, magnetical and mechanical properties [7, 8, 9, 10, 11, 12], incorporation of foreign atoms in tubeles forming metal wires [13, 14] and in possible technological applications as highly performing nanoscale materials and electronic devices [15] (junctions [16], nanocoils [17], field emitters [18] and pinning material in high $T_c$ superconductors [19], ...) This new field has now grown beyond carbon to encompass other materials as well, such as BN fullerenes [20] and nanotubes [21, 22], $BC_3$ and $BC_2N$ [17, 23] nanotubes, GaSe [24] nanotubes, $WS_2$ and $MoS_2$ [25] nanotubes and fullerenes, etc. A general conclusion can be draw from these experimental/theoretical results: all compounds having layered structures in the bulk phase are likely to form nanotubes and fullerene-like structures.

It would be impossible to give a detailed account of progress in this field in just a few pages. Excellent reviews and monographs [7, 8, 9, 10, 11, 12] exist on this topic, and we refer the interested reader to them for an in-depth discussion. Our aim here is more modest; we will focus on just two aspects of nanotube research, which are nevertheless key aspects in their potential for application: their mechanical properties, which will be discussed in Section 10.4, and their electronic properties, discussed in Section 10.5. Given that the carbon-carbon bond in the graphite basal plane (graphene) is one of the strongest chemical bonds known in nature,

and since carbon nanotubes are nothing but seamless graphene cylinders (see Section 10.3), it is not surprising that nanotubes possess extraordinary mechanical properties, a fact that may lead to their use in the fabrication of light but highly resistant fibers, or for the reinforcement of materials, to cite a few examples. With regard to their electronic properties, single-wall nanotubes can be either conducting or semi-conducting, depending on their structure, a property which could be relevant for applications in nano-electronics.

Nanotube research, and in particular the study of the mechanical and electronic properties of nanotubes, is a clear example of a field of study in which the interplay between theoretical studies and experiment has proved to be extremely fruitful.

## 10.2 Theoretical models

In this section we present a brief summary of the theoretical methods we have used to study the mechanical and electronic properties of nanotubes.

In the case of carbon materials with mainly $sp^2$-like bonding the simpler model used is the Tight-Binding (TB) [26] or Hückel model for a $\pi$-bonded graphene sheet [7]. In this model we retain only nearest neighbour interaction between $p_z$-orbitals oriented perpendicularly to the tube axis. The Hamiltonian is $H_{ij}{=}{-}\gamma_0$ for nearest neighbour atoms, and $H_{ij}{=}0$ otherwise and it is known to provide an excellent description of the low energy features for the band structure of isolated armchair nanotubes [27], when $\gamma_0 \sim 2.7$ eV. A brief discussion of how this $\gamma_0$-value depends on the structure of the tube is given in Section 10.5. The main advantage of this model is that can be solved analytically. The wavefunctions of the band states crossing the Fermi level ($k_F = 2\pi/3a$) are $\psi_i(x){=}c_i \sin(kx)$, with $c_1{=}c_2{=}{-}c_3{=}{-}c_4$ for the bonding states (descending band), and $c_1{=}{-}c_2{=}{-}c_3{=}c_4$ for the antibonding solutions. This model turns out to be rather useful in describing the STM images of carbon nanotubes [28, 29, 30, 31].

For the extensive calculations on the mechanical properties we have resorted to a non-orthogonal Tight-Binding [26] scheme due to Porezag and coworkers [32], known as the DFTB model (see Section 10.4). This model has been parametrised for C, B, N as well as for other elements, and is thus well suited for the study of nanotubes. We will not go into details of the model here, but suffice it to say that a DFTB parametrisation is constructed on the basis of DFT calculations employing atomic-like orbitals in the basis set. The non-orthogonality of the basis set is retained, in contrast to the usual practice in empirical TB models, but the approximation of disregarding three-centre contributions to the Hamiltonian matrix elements is used in order to simplify the method. As well as the conventional band-structure contribution to the total energy, the model incorporates a short-range pair-repulsive potential, which is constructed in such a way as to reproduce the DFT results obtained with the same basis in a number of reference systems.

We have performed the *ab-initio* calculations using the standard plane-wave pseudopotential total-energy scheme [33, 34] in the local density approximation (LDA) [35] to the exchange correlation potential. *Ab-initio* norm-conserving nonlocal ionic pseudopotentials have been generated by the soft-pseudopotential method of Troullier and Martins [36]. The LDA wave functions were expanded in plane-waves up to a 48-Ry cutoff (see refs. [33, 34] for details of the method). When studying finite length tubes, the large unit cell together with the large number

of atoms involved ($\simeq 1000$) makes the plane-wave calculation prohibitive. In this case we made calculations in a localized atomic-orbital basis set [37] that has been already applied successfully in studying electronic, structural and STM images of carbon-nanotubes [28, 38].

## 10.3 Nanotube structure

Before discussing in any more detail the mechanical and electronic properties of nanotubes, a brief description of their structure is in order. A nanotube can be regarded as a graphene sheet, i.e. a 2-D array of carbon atoms in a hexagonal pattern, rolled up in such a way as to form a seamless cylinder. This would give the simplest type of nanotube: the single-wall nanotube (SWNT). Often, however, nanotubes are formed by multiple cylindrical shells in a co-axial fashion, with a shell spacing approximately equal to the inter-layer spacing in graphite, namely 3.4 Å. These are known as multi-wall nanotubes (MWNT). Both SW and MWNT share a common feature in that their aspect ratio, that is the ratio of their length to their width, is very large. While the diameter of a SWNT nanotube is usually in the range 1-2 nm, and that of a MWNT nanotube can vary up to 25 nm, their length approaches the $\mu$m scale. Thus, nanotubes are essentially 1-D systems.

Consider a flat graphene sheet, and choose a given atom in the lattice as the origin. A vector with its end at the origin and its tip at any other atom of the same type[1] can be written as $\mathbf{c} = n\mathbf{a}_1 + m\mathbf{a}_2$, where $n$, $m$ are integers and $\mathbf{a}_1$ and $\mathbf{a}_2$ are the lattice vectors. Now, if we take the sheet and cut it along two lines perpendicular to vector $\mathbf{c}$ passing through its tip and its end, and we then fold the graphene band that results in such a way that the tip of vector $\mathbf{c}$ is made to coincide with its end, what results is a nanotube which can be uniquely labeled as (n,m). Nanotubes constructed in this way can be classified into three different kinds: (n,0) nanotubes have atoms arranged in a zig-zag pattern along the circumference of the tube, and are thus called zig-zag nanotubes. (n,n) nanotubes, by contrast, have atoms arranged in an arm-chair pattern. Both zig-zag nanotubes and arm-chair nanotubes are identical to their respective mirror images, and are therefore achiral. General (n,m) (with m$\neq$n$\neq$0) cannot be superimposed on their mirror images, and are therefore chiral nanotubes. From zone-folding symmetry considerations based on the semimetallic band-structure of a single-graphene sheet [27], a tube will be metallic if its values of $n$ and $m$ obey the relation $2n + m = 3q$ where $q$ is an integer; $(n, n + 3i)$ tubes (with $i$ an integer) are small-gap semiconductors with $E_{gap} \propto \frac{1}{R^2}$ and other tubes have larger gaps proportional to $\frac{1}{R}$, being $R$ the radii of the tube. This classification depends critically on the size and location of the graphitic Fermi points.

## 10.4 Mechanical Properties of Nanotubes: the Young's Modulus

The Young's modulus, $Y$, quantifies the resistance that a material opposes against deformation in a particular direction. In particular for nanotubes, it is important to determine the Young's

[1] Since the hexagonal graphene sheet is a lattice with a basis of two atoms, type 1 and type 2 atoms, the end and the tip of the vector must connect two atoms of the same type in the basis.

modulus along the axial direction. $Y$ is usually defined by the following expression:

$$Y = \frac{1}{V_0}\left(\frac{\partial^2 E}{\partial \epsilon^2}\right)_{\epsilon=0}, \tag{1}$$

where $E$ is the total energy, $\epsilon$ is the strain in the direction of deformation and $V_0$ is the equilibrium volume[2].

The Young's modulus of conventional materials varies from a few GPa to up to 600 GPa for the hardest materials, such as diamond and SiC. Since the discovery of nanotubes it was speculated that they could have values of $Y$ even larger than this, given that the in-plane C–C bond in graphite is one of the strongest chemical bonds known in nature (the $c_{11}$ elastic constant in graphite is 1.060 TPa [8]). The first hard evidence in this respect was provided by Treacy *et al.* [39], who, by monitoring the amplitude of the thermal oscillations of the free tips of anchored MWNT's at a range of temperatures, were able to obtain an estimation of their Young's modulus. The mean value of $Y$ obtained was 1.8 TPa, but the data for individual nanotubes ranged from 0.4 to 4.15 TPa, evidence of the large statistical errors in their measurement. Although the value first reported by Treacy and coworkers is now generally accepted to be slightly too large, it is nevertheless indicative of the exceptional mechanical properties of carbon nanotubes.

The same experimental technique has been used by Chopra and Zettl [40] to determine the Young's modulus for BN nanotubes. These authors reported a value of 1.22 TPa. More recently, Krishnan *et al.* [41] have also used this technique to determine the value of $Y$ for carbon SWNT's. Their reported value, 1.25 TPa, is much closer to the expected value for graphite along the basal plane, and is probably a more realistic figure than that obtained earlier by Treacy and coworkers [39].

Wong *et al.* [42] have used a different approach to probe the mechanical properties of nanotubes. They have used an Atomic Force Microscope (AFM) to exert a distortion on the free-standing part of an anchored nanotube, while simultaneously recording the force exerted on the tip by the nanotube as this is being pushed out of its equilibrium position. These authors reported a value of 1.28 TPa for MWNT's, in very good agreement with the results of Krishnan *et al.* [41] for SWNT's. That both SW and MWNT's have very similar Young's modulus is indicative of the fact that the stiffness of nanotubes is essentially a consequence of the strength of the C–C bond in the graphene sheets, the interaction between different walls in MWNT's having only a small effect on their mechanical properties. Other groups have also reported experiments aimed at determining the mechanical properties of nanotubes, such as Salvetat *et al.* [43] and Muster *et al.* [44]. All these experiments have contributed to confirming that nanotubes indeed have exceptional stiffness along the axial direction. Also, there are many direct observations of the large bending flexibility [45, 46] of nanotubes, which provide evidence of their capability to sustain large strains without evidence of collapse or failure. This flexibility property stems from the the ability of the $sp^2$ network to rehybridize when deformed out of plane, the degree of $sp^2 - sp^3$ rehybridization being proportional to the curvature.

[2]For the particular case of a SWNT, $V_0$ is not well defined, since one cannot unambiguously assign a thickness to a shell which is one-atom thick. The conventional way to bypass this problem is to assume a thickness equal to 3.4 Å, i.e. the inter-layer spacing in graphite. This convention is used by experimentalists and theoreticians alike, although it is not universally followed.

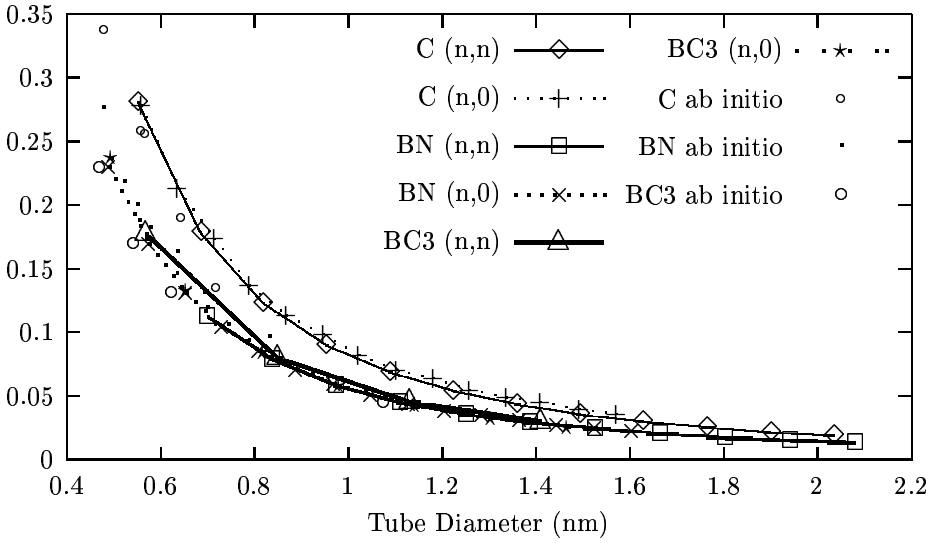


Figure 1: Curvature strain energy as a function of the equilibrium tube diameter, as obtained from the tight-binding calculations, for C, BN and $BC_3$ nanotubes. The strain energy is given in eV/atom.

The mechanical properties of nanotubes have also been investigated by theoretical means [47, 48, 49, 50, 51, 52, 53]. In the majority of cases these studies have been performed using empirical potential models. Well tested empirical potentials exist for carbon based systems, but no such models are generally available, to our knowledge, for other systems such as BN or $BC_3$. It would be possible in principle to study composite nanotube systems by means of first-principles Density Functional Theory (DFT) calculations. Indeed we have carried out such calculations for a small number of nanotubes. However, they are extremely costly, and especially for nanotubes, given that these contain large regions of empty space which nevertheless increase the cost of the calculation significantly. Our approach [54] has thus been to perform DFT calculations in a small number of cases only, and to use these results as a benchmark for calculations using a simpler description of the atomic interactions, namely a Tight-Binding (TB) model [26]. The model of our choice has been the non-orthogonal DFTB scheme proposed by Porezag and co-workers [32]. A point worth stressing is the fact that no fitting to mechanical properties of the system under study is carried out during the parametrisation of the model. Nevertheless the parametrisations that result from this scheme are reliable enough as to predict structural, energetic and mechanical properties which are in very good agreement with both empirical data and results from higher levels of theory (first-principles DFT), as will become apparent below.

Before describing our theoretical calculations of the Young's modulus let us consider the concept of *strain energy* of nanotubes, i.e. the energy difference between a nanotube and its parent flat graphene structure. Fig. (1) shows the strain energy for tubes of different composition as a function of the tube diameter, calculated by means of the DFTB model and from first-principles DFT calculations [14, 17, 22]. Notice the good agreement that can be observed between the first-principles and the DFTB results, which serves as a first indication that the DFTB model is capable of giving a good description of the energetics of nanotubes of different chemical composition. It can also be seen that carbon nanotubes are predicted to have the highest strain

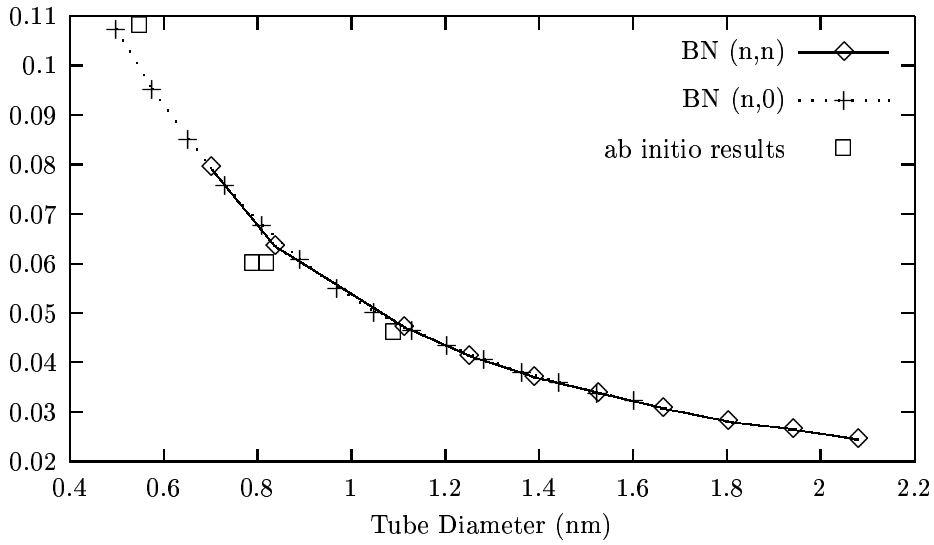


Figure 2: Buckling in the BN nanotube equilibrium structures vs. tube diameter. We define the buckling as the mean radius of the nitrogen atoms minus the mean radius of the boron atoms, and is given in Å.

energy at all tube radii. In fact, this is already an indication that carbon nanotubes have a higher Young's modulus than any of the composite nanotubes considered here. Tibbets [55] has shown that the strain energy in the continuum elasticity theory limit is given by

$$E_s = \frac{Ya^3}{6}\frac{\Omega}{D^2}, \tag{2}$$

where $E_s$ is the strain energy per atom, $Y$ is the Young's modulus, $a$ is a constant of the order of the inter-layer spacing in graphite, $\Omega$ is the area per atom and $D$ is the tube diameter. According to this expression, types of nanotubes with higher strain energy should have a higher Young's modulus. Fitting the data of Fig. (1) to an expression of the form $\alpha D^{-\beta}$ shows that the calculated strain energy obtained for the different types of tubes considered here follows very closely the behaviour predicted by Tibbets.

Another indication of the reliability of the DFTB model used in the present study is its ability to reproduce rather fine structural details of these tubular systems predicted from plane-wave DFT pseudopotential calculations [22]. These calculations predict that BN nanotubes are slightly buckled on the surface; the B atoms displace inwards towards the tube axis, while the N atoms displace in the outward direction. The amount of buckling is dependent on the tube diameter, but it is otherwise independent of the tube structure, as can be seen in Fig. (2). This figure also shows the results obtained from the DFT calculations [22], and it can be seen that the agreement between both calculations is rather good.

Finally, let us consider the direct evaluation of the Young's modulus from DFTB calculations. Results for selected nanotubes of the different compositions considered are given in Table. (1). Each tube considered has been simulated as an infinitely long nanotube using periodic boundary conditions along the tube axis. A series of calculations were performed for each tube, varying the length of the repeat cell and relaxing the atomic positions without constraints. From these calculations we obtain the equilibrium configuration as well as stressed configurations, which

| $B_xC_yN_z$ | (n,m) | $D_{eq}$ (nm) | $\sigma$ | $Y_s$ (TPa · nm) | $Y$ (TPa) |
|---|---|---|---|---|---|
| C | (10,0) | 0.791 | 0.275 | 0.416 | 1.22 |
| | (6,6) | 0.820 | 0.247 | 0.415 | 1.22 |
| | | (0.817) | | (0.371) | (1.09) |
| | (10,5) | 1.034 | 0.265 | 0.426 | 1.25 |
| | (10,7) | 1.165 | 0.266 | 0.422 | 1.24 |
| | (10,10) | 1.360 | 0.256 | 0.423 | 1.24 |
| | (20,0) | 1.571 | 0.270 | 0.430 | 1.26 |
| | (15,15) | 2.034 | 0.256 | 0.425 | 1.25 |
| BN | (10,0) | 0.811 | 0.232 | 0.284 | 0.837 |
| | (6,6) | 0.838 | 0.268 | 0.296 | 0.870 |
| | | (0.823) | | (0.267) | (0.784) |
| | (15,0) | 1.206 | 0.246 | 0.298 | 0.876 |
| | (10,10) | 1.390 | 0.263 | 0.306 | 0.901 |
| | (20,0) | 1.604 | 0.254 | 0.301 | 0.884 |
| | (15,15) | 2.081 | 0.263 | 0.310 | 0.912 |
| $BC_3$ | (5,0) | 0.818 | 0.301 | 0.308 | 0.906 |
| | (3,3) | 0.850 | 0.289 | 0.311 | 0.914 |
| | (10,0) | 1.630 | 0.282 | 0.313 | 0.922 |
| | (6,6) | 1.694 | 0.279 | 0.315 | 0.925 |

Table 1: Structural and elastic properties of selected nanotubes obtained from the tight-binding calculations reported here. Young modulus values given in parenthesis were obtained from first-principles calculations. Also the value of $Y$ with the convention $\delta R = 0.34$ nm is given for comparison. Values given in parenthesis were obtained from plane-wave DFT-pseudopotential calculations, and are given for comparison.

give us the total energy as a function of the imposed axial strain. From this data we are able to obtain the Young's modulus using Eq. (1). The results we obtained, given in Table (1), were obtained using the normal convention of taking the wall-thickness equal to 3.4 Å.

It can be seen from Table (1) that indeed the carbon nanotubes have the highest Young's modulus, as predicted from Tibbet's formula [55] for the strain energy. The BN and $BC_3$ tubes have similar values of the Young's modulus, around 0.9 TPa, which is less stiff than that of the pure carbon nanotubes, but still considerably stiff. The tubes of $BC_2N$ composition have Young's modulus in between the C and $BN/BC_3$ nanotubes, having a value around 1 TPa. Although tubes of $BC_2N$ composition have been synthesized, it now appears to be the case that these consist of concentric shells of C and BN, with pure C nanotubes in the inner and outer shells, and BN in the middle; stoichiometrically homogeneous $BC_2N$ tubes have not been yet obtained, to our knowledge.

The value of the Young's modulus obtained for the wider carbon nanotubes is 1.26 TPa, which is in very good agreement with the experimental value reported by Krishnan *et al.* [41] (1.25 TPa) for SWNT's, and also with the value obtained by Wong *et al.* [42] (1.28 TPa) for MWNT's. As we have pointed out earlier, the fact that SW and MWNT's are reported to have very similar

values of Y is not surprising, as we expect Y to be mostly determined by the strength of the C–C bond in the graphene sheets. For the composite nanotubes, the only existing experimental data is that of Chopra and Zettl [40] for BN nanotubes. They quote a value of 1.22 TPa, slightly larger than what we obtain (0.9 TPa for the widest tubes), but still within reasonably good agreement. For the particular case of the (6,6) C and BN nanotubes, plane-wave DFT pseudopotential calculations were also carried out for comparison. The results obtained from these benchmark calculations are also shown in Table (1). Notice the good agreement between these and the DFTB results.

More recently we have also reported results for $C_3N_4$ nanotubes [56]. Although nanotubes containing C and N have been synthesized [57], it has not yet been possible to obtain structures of $C_3N_4$ stoichiometry. The presence of N in these structures seems to prevent graphitisation [58], in contrast to what happens when B is present [59]. Nevertheless, since it has been speculated in the past that CN structures could lead to ultra-hard materials [60], we have considered the $C_3N_4$. Our results indicate that such tubes would be significantly softer than the other tubes considered earlier, having a Young's modulus of the order of 0.6 TPa.

### 10.5 Density-of-states: STS-spectroscopy

The relation between nanotube chirality and its electrical properties can be complementary explored by theoretical calculations and Scanning Tunneling Microscopy (STM) experiments, since it allows both topographic imaging and Scanning Tunneling Spectroscopy (STS) from which information about the local density of states (LDOS) can be obtained. STM have resolved the atomic structure and confirmed the predicted interplay between geometry and electronic properties [61, 62, 63]. However, the determination of the diameter of the nanotube is not straightforward due to tip-convolution effects and operation mode. The chiral angle can be affected by mechanical distortions [64] and by the geometry of the STM experiment in obtaining the topographic image: the cylindrical geometry of the nanotube produces a geometrical distortion of the image stretched in the direction perpendicular to the tube axis [31]. Interactions stemming from tube-packing or tube/substrate/tip can modify the predicted properties of isolated SWNT and need further study and detailed analysis [28, 29, 30].

The DOS gives a direct information about the metallic/semiconducting behaviour of the nanotubes as well as particular insight into the tube-tube or tube-substrate interactions. Information about structural properties and local environment for a carbon or composite nanotube can be extracted from the computed DOS [30]. In a recent work, the connection between tube-diameter and low-energy features in the DOS has been pointed out[65, 66]. The fact that the electronic DOS for each metallic or semiconducting tube is practically independent of the nanotube chirality, is in qualitative agreement with STS experiments [61]. The simple $\pi$-electron TB model was used to get this general correlation between tube-diameter and features in the DOS [65, 66] (see below for more details about this model in comparison with first-principles calculations). We have shown [29] that curvature induced $\sigma$-$\pi$ hybridisation leads to quantitative changes in the DOS in both peak energies and intensities. Therefore, the TB-results are only valid for states a few tenths of an eV above or below the Fermi level, and ab-initio calculations

are needed to address the validity of this simple model and to get a meaningful comparison with experiments.

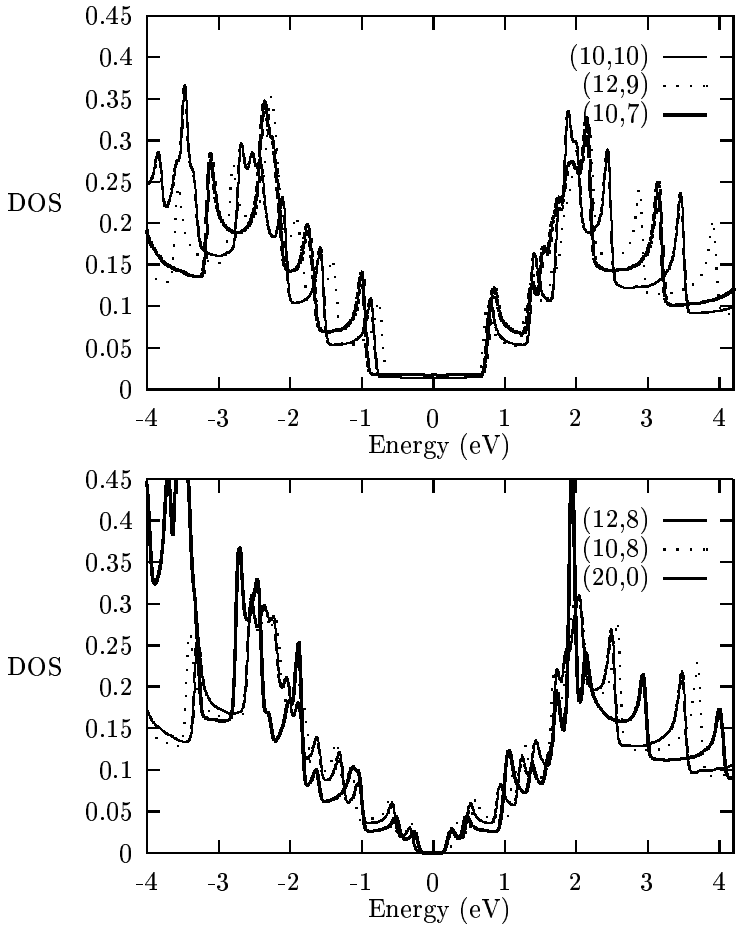


Figure 3: Ab initio DOS for different metallic (top panel) and semiconducting (bottom panel) tubes with diameters in the range of 1-2 nm, namely: 1.17, 1.36, 1.44, 1.23, 1.37 and 1.58 nm for the (10,7), (10,10), (12,9), (10,8), (12,8) and (20,0) nanotubes, respectively. Spikes in the DOS stems from the van Hove singularities of the nanotube 1D-band-structure. All DOS are normalized to the number of atoms in the nanotube unit cell.

In Fig. (3) we plot the computed ab-initio DOS for a set of chiral and non-chiral tubes with diameters around the experimental value of 1.3 nm (between 1.1 and 1.6 nm). The following conclusions can be extracted from the figure:

(i) in metallic tubes the plateau around the Fermi level depends on both tube diameter and, to a lesser extent, on tube-chirality. For almost all tubules with $\sim$1.3 nm diameter the metallic-plateau is about 1.7-2.0 eV. This data is of importance is discriminating metallic and semiconducting tubes in resonant-Raman scattering experiments [67, 68]. The non-armchair tubes belonging to the metallic group are indeed quasimetallic with an extremely small gap introduced at the Fermi level by curvature effects.

(ii) The electron-hole symmetry of the TB-model is no longer valid even for the first spikes in the DOS (see the clear example of the (10,7) metallic tube). This effect gets more clear as the nanotube radius is reduced or/and as we move away from the Fermi level. The

separation between van Hove singularities is also slightly different for both conduction and valence states.

(iii) The direct connection between the diameter and the structure of the spikes in the DOS is not always clear. Note for example that the semiconducting (12,8) and (20,0) nanotubes have very similar DOS close to the Fermi level. However their diameters are 1.37 and 1.58 nm, respectively. The same holds for the metallic (12,9) and (10,10) tubes with very similar "metallic-plateau", but diameters of 1.44 and 1.36 nm, respectively. Then, although the proposal in ref. [65] is very appealing, its practical application to discern the tube-diameter is doubtful in its spatial resolution (not better than 0.15 nm for the diameter).

To get insight into tube-tube interaction in MWNT we plot in Fig. (4) the DOS for a MWNT formed by three concentric armchair tubes such that the inter-tube distance is close to the graphitic value and for a bundle or nanotube-rope constituted by three (8,8) SWNT packed on an equilateral triangle network with 0.345 nm intertube distance. In the MWNT case we see that the low-energy structure seems to give information about the number of layers in the tube, however this identification gets more complicated when non-commensurate metallic or semiconducting tubes participate as main building blocks of the MWNT. As expected, the metallic-plateau of the MWNT is mainly controlled by the outer tube. The interaction among tubes being weak, only shifts a little bit the position of the van Hove singularities in the MWNT with respect to the SWNT. This shift is larger for the conduction states making the electron-hole asymmetry more clear. In the case of the nanotube bundle the interaction clearly modifies the spectra seen in the DOS in the following way:

(i) It opens a "pseudogap" close to the Fermi level as already predicted for random oriented nanotube ropes[69] (pseudogap of $\sim 0.1$ eV). The bundle remains metallic.

(ii) It makes the electron-hole asymmetry in the DOS more accentuated and the spike structure of the van Hove singularities is smoothed out.

The fact that the position in energy of the peaks is not strongly modified explains the success of using isolated SWNT spectra to describe the experimental data [61]. However the shape of the spectra (relative intensities) is strongly affected by tube-tube interactions.

It is worth discussing these results in terms of the simple $\pi$-electron TB model. The hamiltonian in this case has electron-hole symmetry around the Fermi level and the DOS can be expressed in terms of a universal function that depends only on whether the tube is metallic or semiconducting [65]. In terms of the nearest neighbour overlap energy $\gamma_0$ we have that, for a semiconducting tube, the band-gap is given by

$$E_g = \frac{2\gamma_0 a_{C-C}}{D} \, , \tag{3}$$

where $a_{C-C}$ is the carbon-carbon bond-length ($\sim 1.42$Å) and $D$ is the nanotube diameter. In the case of metallic tubes, the metallic plateau ($E_{met}$), given by distance between the two van Hove singularities above and below the Fermi level, is

$$E_{met} = \frac{6\gamma_0 a_{C-C}}{D} \, . \tag{4}$$

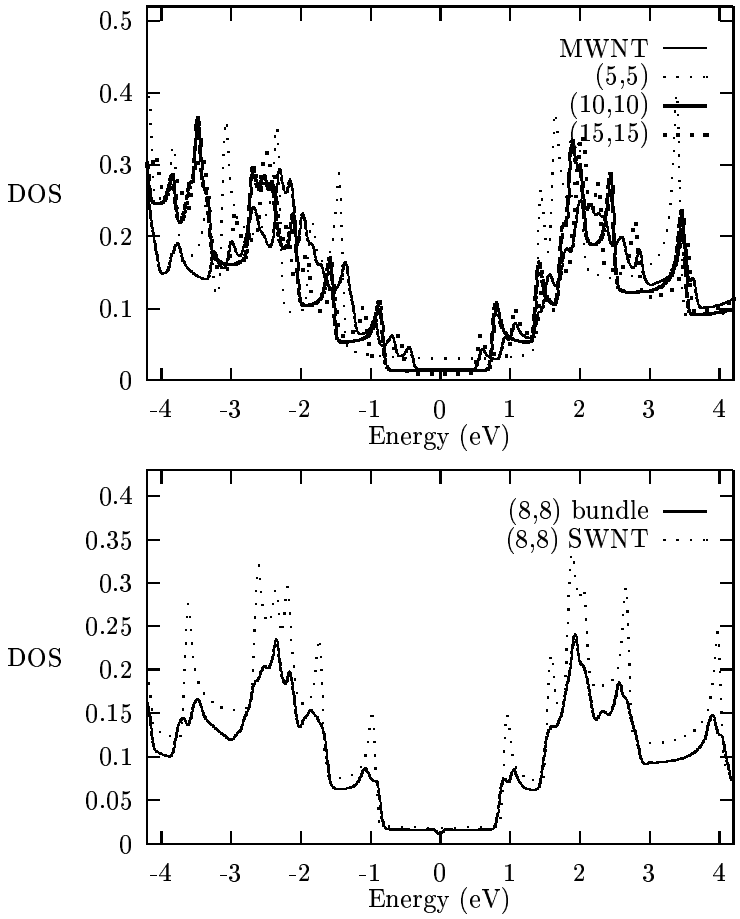


Figure 4: Top panel: DOS for a MWNT formed by three concentric armchair tubes: (5,5)+(10,10)+(15,15). Bottom panel: DOS for a small nanotube-rope (bundle) formed by three (8,8) SWNT (1.09 nm diameter) packed in a triangular lattice with an intertube distance of 0.345 nm. We clearly see the opening of a "pseudogap" of about ∼0.1 eV around the Fermi level. We compare the results for the bundle with the DOS for an isolated (8,8) SWNT (dashed line). Each DOS is normalized to the number of atoms in the unit cell.

In both cases the distance between consecutive conduction or valence van Hove singularities is given by

$$\Delta E = \frac{3\gamma_0 a_{C-C}}{D} \, . \tag{5}$$

This $\gamma_0$ parameter plays an important role in the experimental analysis of their electronic structure data. In fact, a fit to STS experiments [61] give a value of $\gamma_0$=2.7 eV, whereas the fit to resonant Raman scattering experiments on metallic carbon nanotubes [68] gives $\gamma_0$=2.95±0.05 eV. This indirect estimation is in quite good agreement with the direct measurement by STS, and both are smaller than the $\gamma_0$=3.16 eV value for graphite [8]. Our results show that the value of $\gamma_0$ is not unique due to the anisotropy of the DOS in both peak positions and intensities. Semiconducting tubes are the best candidates to extract experimentally the value of $\gamma_0$ from eqn. (3). We got values from 2.77 to 2.95 eV for tubes with diameters of 1.23 and 1.58 nm, respectively. Smaller values are obtained for metallic tubes when fitting the metallic plateau to eqn. (4) (from 2.32 to 2.75 eV for diameters of 0.68 to 2.04 nm, respectively). In general, the value of $\gamma_0$ increases with increasing nanotube diameter and the

interaction between tubes also modify this parameter by as much as 10% [29]. In fact, the electron-hole asymmetry in the density of states is a measure of the curvature effects, intertube interactions and anisotropy in the band-structure.

As most STM experiments are performed on supported tubes on substrates [62, 63], therefore it is important to get insight about the role played by the substrate in the experimental images. We have shown [28], in the case of the experimentally supported tubes on Au(111), that the gold substrate modifies the spectrum in several ways.

(i) It opens a small "pseudogap" in the tube states at the Fermi level whenever the symmetries of the tube are not respected by the gold substrate [69]

(ii) It shifts the Fermi level, producing a transfer from the gold to the nanotube and a quite strong tube-substrate bonding that prevents the tube from moving.

However, even if the electronic level structure is very sensitive to external perturbation, we have found [28, 29] that the whole set of STM images of armchair carbon nanotubes can be understood in terms of the isolated SWNT wave-functions that, in the simple TB-model, offers a catalog of just four image patterns [28] (this result is confirmed by ab-initio calculations).

### 10.6 Finite-size effects

The study of electron standing-wave (SW) in nanostructures is of fundamental interest as one addresses directly theoretical and experimental problems connected with low-dimensional systems (an example are the nanotubes as quasi one-dimensional-molecular wires). Typical aspects of the nanoscale world as Coulomb blockade, localization, oscillations in the conductivity and the quantized conductance (in units of the conductance quantum $G_0 = 2e^2/h$=(12.9 kiloohms)$^{-1}$) of nanotubes have been already observed[15, 70, 71]. In this last case, the nanotubes conduct current ballistically and do not dissipate heat. In fact, conduction electrons in armchair nanotubes have very large electron mean free paths resulting in exceptional ballistic transport and localization lengths of 10$\mu$m [72].

The transition from a one-dimensional (1D) to a zero-dimensional (0D quantum-dot) system can be studied by looking at different finite-length carbon nanotubes[28, 62]. More detailed information about the electronic structure of 1D-quantum wires can be directly obtained in STS experiments by mapping the 1D-confinement of electrons in the nanotube structure. This can be achieved by cutting the tube to a finite-length [73], which reduces the periodic band-structure to a discrete set of molecular levels[74] that can now be imaged by STM [62, 75]. In this simple scenario of a 1D particle-in-a-box model, a tube of length $L$ has a set of allowed k's given by $k = n\pi/L$ ($n$ integer). Taking the Fermi level of the tube at the single graphene-sheet value of $k_F = \frac{2\pi}{3a}$, the wavefunctions close to the Fermi level will exhibit a periodic pattern with a wavelength of $\lambda_F = 3a = 0.74$ nm, as observed in STS measurements [62]. Although, this basic standing wave observation can be explained in terms of the simple 1D particle-in-a-box model, further insight is needed to understand their energy and three-dimensional shape [28]. Evidence for 1D quantum confinement was already obtained from transport measurements on single-wall

tubes [70, 76], but the standing-wave states have been observed only recently in 1D scans of scanning tunneling spectroscopy (STS) [62] and described theoretically[28].

In general, the value of the HOMO-LUMO gap decreases with increasing tube length not monotonically but exhibiting a well defined oscillation that is related to the localization and bonding character of the HOMO and LUMO orbitals [3]. By increasing the tube-length we observe a smooth transition from an energy level structure characteristic of a molecular-wire (0D-system) to that of a delocalized one-dimensional system, that seems to be complete for tube-lengths of the order or larger than 5 nm [74].

Furthermore, the geometry of the nanotube-cap give rise to localized states close to the fermi level [63, 77]. The spatial localization and expected coherent electron emission of these states, makes this finite capped nanotubes ideal candidates for the scanning microscopy tip and electron emission materials [18]

### 10.6.1 STS on Boron-Nitride nanotubes

The electronic properties of BN nanotubes are quite different to carbon, namely: all are stable wide band-gap semiconductors independent of helicity and diameter of the nanotube and of whether the nanotube is single- or multi-walled. The band-gap constancy may be of importance for technological applications because samples containing many different sizes could be grown with predictable electronic properties even in the multiwall case playing an important role in applications involving $n$-type doping. The existence of NFE-states above $E_F$ is systematically seen in the C-, $BC_3$-, $BC_2N$-sheets and tubules but are much higher in energy than for the BN-systems and do not play an important role in their electronic properties as does for BN [22, 78].

In Fig. (5) we present our preliminary data on the spectroscopic properties of BN-nanotubes. The aim is to look for a general behaviour of the van Hove singularities as a function of tube diameter and chirality. In contrast to carbon nanotubes, the first spikes provides us with the semiconducting band-gap that is rather insensitive to tube chirality and diameter. Furthermore, the structure and intensities of the next spikes in the DOS depends clearly not only on the diameter but also on the structural geometry. We are presently working in trying to rationalize this results in terms of a simple parametrised TB model for BN [22] and to describe a general chiral nanotube.

## 10.7 Conclusions

To summarise our results on the mechanical properties of nanotubes, we have used the non-orthogonal TB scheme of Porezag and coworkers [32] known as DFTB to study the structural, energetic and mechanical properties of nanotubes of $B_xC_yN_z$ composition, obtaining rather good agreement with the available experimental data, as well as with results from DFT calculations. Our results indicate that C nanotubes are very stiff, the stiffest of the different nanotubes

[3]The band-gap behavior can be divided in four classes depending of the tube length, chirality and capping geometry: (i) the gap diminished toward the infinite-tubule value with a period-3 oscillation of amplitude quenched as 1/L; (ii) the gap diminished monotonically as 1/L to the infinite value; (iii) the gap approaches exponentially fast a constant value different than that for the infinite tubule and (iv) the gap is constant [74].

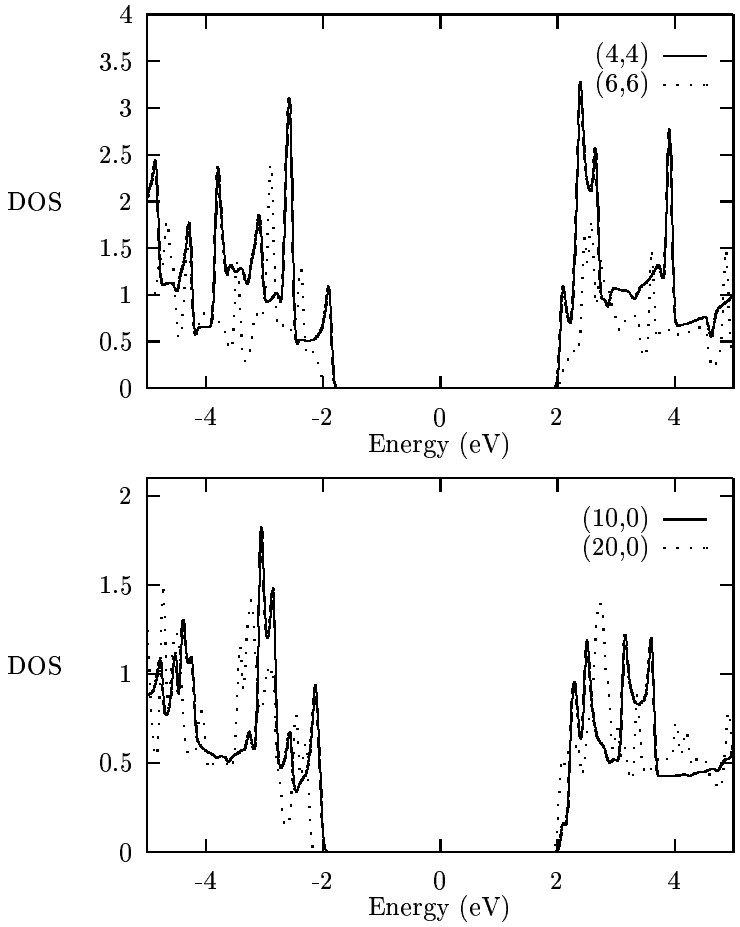


Figure 5: Up: Calculated DOS for SWNT's made of BN. Top panel corresponds to armchair nanotubes and bottom panel to zig-zag nanotubes. The band-gap is less sensitive to chirality and diameter than the peak-structure in the DOS.

considered, having a Young's modulus of approximately 1.26 TPa at the diameter range found in experimental samples of SWNT's (1.3 nm). We indicate that the flexibility of composite nanotubes during bending in a wide range of practical conditions shows substantial promise for structural, fiber applications ( the "ultimate" lightweight-high-strength flexible fiber) and nanotube-reinforced materials. This is due to the remarkable flexibility of the hexagonal network, which resist bond breaking and bond switching up to very high strain values. One direct application is related to the atomic-force microscope (AFM). Carbon nanotubes have previously been used as tips in AFM for producing images [79]. Now for the first time nanotube tips have been used as pencils for writing 10-nm-width structures on silicon substrates [80].

The combination of the spectroscopic models developed in the last section for carbon and boron-nitride can be extended to get information about the structural properties of the recent synthesized sandwiches of carbon and boron nitride nanotubes [81]. This structures have is mainly formed by carbon layers at the center and at the periphery, separated by few BN-layers. Further developments of multielement nanotubes forming this type of coaxial "nanocable" structure has been achieved [82]. This new structure resembles a coaxial nanocable with semiconductor-insulator-metal/semiconductor geometry and it is made of silicon carbide at the

core of the nanowire covered by an amorphous layer of silicon oxide. The whole structure is sheathed by graphitic layers of carbon and boron-nitride. This new type of structures could have technological applications.

In summary, more striking advances both in theory and experiments are ready to come in the near future, as can be expected from the tremendous advances in the field in the last years. We have to be ready to discover some "surprises" to stem from the new physical and chemical properties of this whole class of nanocomposite materials.

### 10.8 Acknowledgments

We acknowledge financial support from JCyL (Grant: VA28/99), DGES (Grants: PB95-0720 and PB95-0202) and European Community TMR contract ERBFMRX-CT96-0067 (DG12-MIHT). Computer time was provided by the $C^4$ (Centre de Computació i Comunicacions de Catalunya). We thank C. Dekker, L.C. Venema and D.L. Carrol for sharing their experiments with us prior to publication and for enlightening discussions. We also benefited from fruitful collaborations with J.A. Alonso, E. Artacho, P. Bernier, C. Goze, Ph. Lambin, M.J. López, V. Meunier, P. Ordejón, D. Sánchez-Portal and J.M. Soler.

## References

[1] H.W. Kroto, J.R. Heath, S.C. O'Brien, R.F. Curl and R.E. Smalley, Nature **318**, 162 (1985).

[2] W. Krätschmer, L.D. Lamb, K. Fostiropoulos and D.R. Huffman, Nature **347**, 354 (1990).

[3] S. Iijima, Nature **354**, 56 (1991); P.M. Ajayan and S. Iijima, Nature **361**, 333 (1993); Iijima and T. Ichihashi, Nature **363**, 603 (1993); D.S. Bethune, *et al.*, Nature **363**, 605 (1993).

[4] W. Marx, M. Wanitschek and H. Schier, in *Electronic Properties of Novel Materials – Progress in Molecular Nanostructures*, H. Kuzmany, J. Fink, M.Mehring and S. Roth (Eds.), AIP Conference Proceedings Vol. 442, Woodbury NY (1998).

[5] A. Thess, R. Lee, P. Nikolaev, H. Dai, P. Petit, J. Robert, C. Xu, Y.H. Lee, S.G. Kim, A.G. Rinzler, D.T. Colbert, G.E. Scuseria, D. Tomanek, J.E. Fisher, R.E. Smalley, Science **273**, 483 (1996)

[6] C. Journet, W. Maser, P. Bernier, A. Loiseau, P. Deniard, S. Lefrant, R. Lee, J. Fischer, Nature **388**, 756 (1997).

[7] Special issue on *Nanotubes* in Carbon **33** (1996); J. Appl. Phys. A **67** (1998).

[8] M.S. Dresselhaus, G. Dresselhaus, P.C. Eklund, Science of Fullerenes and Carbon Nanotubes (Academic Press Inc., San Diego, 1996).

[9] T.W. Ebbesen, Carbon nanotubes: preparation and properties (CRC Press, New York, 1997).

[10] A. Rubio, Cond. Matt. News **6**, 6 (1997) and references therein.

[11] M. Terrones, W.K. Hsu, H.W. Kroto and D.R.M. Walton, Topics in Current Chemistry **199** 189 (1999).

[12] P.M. Ajayan and T.W. Ebbesen, Rep. Prog. Phys. **60** 1025 (1997).

[13] P.M. Ajayan and S. Iijima, Nature **361**, 333 (1993). C. Guerret-Plécourt, Y. Lebouas, A. Loiseau and H. Pascard, Nature **372**, 761 (1994); M. Terrones *et al*, Appl. Phys. A **66**, 1 (1998).

[14] Y. Miyamoto, A. Rubio, X. Blase, M.L. Cohen and S.G. Louie, Phys. Rev. Lett. **74**, 2993 (1995); A. Rubio, Y. Miyamoto, X. Blase, M.L. Cohen and S.G. Louie, Phys. Rev. B **53**, 4023 (1996).

[15] P.G. Collins, A. Zettl, H. Bando, A. Thess, R.E. Smalley, Science, **278**, 100 (1997); S.J. Tans, A.R.M. Verschueren, C. Dekker, Nature, **393** 49 (1998).

[16] L. Chico *et al.*, Phys. Rev. Lett. **76**, 971 (1996); J.C. Charlier, Phys. Rev. B **53**, 11108 (1996); R. Saito *et al.*, Phys. Rev. B **53**, 2044 (1996).

[17] Y. Miyamoto, A. Rubio, S.G. Louie, and M.L. Cohen, Phys.Rev.B **50**, 4976 (1994); Phys. Rev. Lett. **76**, 2121 (1996).

[18] W.A. de Heer, *et al.* Science **270**, 1179 (1995); Science **268**, 845 (1995); A.G. Rinzler, *et al.* Science **269**, 1550 (1995); S. Fan, M.G. Chapline, N.R. Frankling, T.W. Tombler, A.M. Cassell and H. Dai, Science **283**, 512 (1999).

[19] T.W. Ebbesen, Physics Today **49**, 26 (1996)

[20] L. Boulanger, B. Andriot, M. Cauchetier and F. Willaime, Chem. Phys. Letts. **234**, 227 (1995)

[21] N.G. Chopra, R.J. Luyken, K. Cherrey, V.H. Crespi, M.L. Cohen, S.G. Louie and A. Zettl, Science **269** 966 (1995); A. Loiseau, F. Willaime, N. Demoncy, G. Hug and H. Pascard, Phys. Rev. Lett. **76** 4737 (1996) M. Terrones *et al.*, Chem. Phys. Lett. **259** 568 (1996); Chem. Phys. Lett. **257** 576 (1996).

[22] A. Rubio, J.L. Corkill and M.L. Cohen, Phys. Rev. B **49** 5081 (1994); X. Blase, A. Rubio, S.G. Louie and M.L. Cohen, Europhys. Lett. **28**, 335 (1994).

[23] Z. Weng-Sieh, K. Cherrey, N.G. Chopra, X. Blase, Y. Miyamoto, A. Rubio, M.L. Cohen, S.G. Louie, A. Zettl and R. Gronsky, Phys. Rev. B, **51** 11229 (1995);O. Stephan, P. M. Ajayan, C. Colliex, P. Redlich, J. M. Lambert, P. Bernier, and P. Lefin, Science **266**, 1683 (1994)

[24] M. Côté, M.L. Cohen and D.J. Chadi, Phys. Rev. B **58**, 4277 (1998).

[25] R. Tenne, L. Margulis, M. Genut and G. Hodes, Nature **360** 444 (1992); R. Tenne, Adv. Mater. **7**, 965 (1995); and references therein.

[26] For a review on tight-binding see C.M. Goringe, D.R. Bowler and E. Hernández, Rep. Prog. Phys. **60** 1447 (1997).

[27] N. Hamada, S. Sawada, A. Oshiyama, Phys. Rev. Lett. **68**, 1579 (1992); W. Mintmire, B.I. Dunlap, C.T. White, Phys. Rev. Lett. **68**, 631 (1992)

[28] A. Rubio, D. Sanchez-Portal, E. Artacho, P. Ordejón and J.M.Soler, Phys. Rev. Lett. (in press).

[29] A. Rubio, Appl. Phys. A **68** (1999)

[30] E. Hernández, A. Rubio (work in progress).

[31] V. Meunier, Ph. Lambin, Phys. Rev. Lett. **81**, 5588 (1998).

[32] D. Porezag, T. Frauenheim, T. Köhler, G. Seifert and R. Kashner, Phys. Rev. B **51** 12947 (1995); J. Widany, T. Frauenheim, T. Köhler, M. Sternberg, D. Porezag, G. Jungnickel and G. Seifert, Phys. Rev. B **53** 4443 (1996); F. Weich, J. Widany, T. Frauenheim and G. Seifert (private communication).

[33] M.L. Cohen, Solid Stat. Commun. **92**, 45 (1994); Phys. Scri. **1**, 5 (1982). J. Ihm, A. Zunger, M.L. Cohen, J. Phys. C **12**, 4409 (1979).

[34] W.E. Pickett, Comput. Phys. Rep. **9**, 115 (1989); M.C. Payne, M.P. Teter, D.C. Allan, T.A. Arias, J.D. Joannopoulos, Rev. Mod. Phys. **64**, 1045 (1992).

[35] D.M. Ceperley, B.J. Alder, Phys. Rev. Lett. **45**, 1196 (1980). J.P. Perdew, A. Zunger, Phys. Rev. B **23**, 5048 (1981).

[36] N. Troullier, J.L. Martins, Solid State Commun. **74**, 613 (1990); Phys. Rev. B **43**, 1993 (1991).

[37] D. Sánchez-Portal, P. Ordejón, E. Artacho, J.M. Soler, Int. J. Quantum Chem. **65**, 453 (1997); P. Ordejón, E. Artacho, J.M. Soler, Phys. Rev. B **53**, R10441 (1996).

[38] D. Sánchez-Portal, E. Artacho, J.M. Soler, A. Rubio and P. Ordejón, Phys. Rev. B (in press 1999).

[39] M.M.J. Treacy, T.W. Ebbesen and J.M. Gibson, Nature **381** 678 (1996)

[40] N.G. Chopra and A. Zettl, Solid State Comm. **105** 297 (1998).

[41] A. Krishnan, E. Dujardin, T.W. Ebbesen, P.N. Yanilos and M.M.J. Treacy, Phys. Rev. B **58**, 14013 (1998).

[42] E.W. Wong, P.E. Sheehan and C.M. Lieber, Science **277** 1971 (1997).

[43] J.P. Salvetat, G.A.D. Briggs, J.M. Bonard. R.W. Bacsa, A.J. Kulik, T.Stōckli, N.A. Burnham and L. Forró, Phys. Rev. Lett **82**, 944 (1999).

[44] J. Muster, M. Burghard, S. Roth, G.S. Düsberg, E. Hernández and A. Rubio, J. Vac. Sci. Tech. **16**, 2796 (1998).

[45] S. Iijima, C. Brabec, A. Maiti and J. Bernholc, J. Chem. Phys. **104** 2089 (1996).

[46] M.R. Falvo, G.J. Clary, R.M. Taylor, V. Chi, F.P. Brooks, S. Washburn and R. Superfine, Nature **389**, 582 (1997); T. Hertel, R. Martel and P. Avouris, J. Phys. Chem. B **102**, 910 (1998)

[47] D.H. Robertson, D.W. Brenner and J.W. Wintmire, Phys. Rev. B **45** 12592 (1992).

[48] R.S. Ruoff and D.C. Lorents, Carbon **33** 925 (1995).

[49] J.M. Molina, S.S. Savinsky and N.V. Khokhriakov, J. Chem. Phys. **104** 4652 (1996).

[50] B.I. Yakobson, C.J. Brabec and J. Bernholc, Phys. Rev. Lett. **76** 2411 (1996).

[51] M.B. Nardelli, B.I. Yakobson and J. Bernholc, Phys. Rev. B **57**, 4277 (1998).

[52] C.F. Cornwell and L.T. Wille, Solid State Comm. **101** 555 (1997).

[53] J.P. Lu, Phys. Rev. Lett. **79** 1297 (1997).

[54] E. Hernández, C. Goze, P. Bernier and A. Rubio, Phys. Rev. Lett. **80** 4502 (1998).

[55] G.G. Tibbetts, J. Cryst. Growth, **66**, 632 (1983).

[56] E. Hernández, C. Goze, P. Bernier and A. Rubio, Appl. Phys. A **68** 287 (1999).

[57] M. Terrones, P. Redlich, N. Colbert, S. Trasobares, W.K. Hsu, H. Terrones, Y.Q. Zhu, J.P. Hare, C.L. Reeves, A.K. Cheetham. M. Rühle, H.W. Kroto and D.R.M. Walton, Adv. Mater. (in press 1999).

[58] J.T. Hu, P.D. Yang and C.M. Lieber, Phys. Rev. B **57** 3185 (1998).

[59] M. Terrones, W.K. Hsu, H. Terrones, J.P. Zhang, S. Ramos, J.P. Hare, R. Castillo, K. Prasides, A.K. Cheetham, H.W. Kroto and D.R.M. Walton, Chem. Phys. Lett. **259** 568 (1996); M. Terrones, A.M. Benito, C. Manteca-Diego, W.K. Hsu, O.I. Osman, J.P. Hare, D.G. Reid, H. Terrones, A.K. Cheetham, K. Prasides, H.W. Kroto and D.R.M. Walton, Chem. Phys. Lett. **257** 576 (1996).

[60] M.L. Cohen, Phys. Rev. B **32**, 7988 (1985); Science **261**, 307 (1993).

[61] J.W.G. Wildöer, L.C: Venema, A.G. Rinzler, R.E. Smalley, C. Dekker, Nature **391**, 59 (1998); T.W. Odom, J.-L. Huang, P. Kim, C.M. Lieber, Nature **391**, 62 (1998).

[62] L.C. Venema, J.W.G. Wildöer, S.J. Tans, J.W. Janssen, L.J. Hinne, T. Tuinstra, L.P. Kouwenhoven, C. Dekker, Science, **283**, 52 (1999).

[63] P. Kim, T.W. Odom, J.L. Huang and C.M. Lieber, Phys. Rev. Lett. **82**, 1225 (1999).

[64] W. Clauss, D.J. Bergeron, A.T. Johnson, Phys. Rev. B **58**, R4266 (1998).

[65] C.T. White, J.W. Mintmire, Nature **394**, 29 (1998); J.W. Mintmire, C.T. White, Phys. Rev. Let. **81**, 2506 (1998).

[66] J.C. Charlier, Ph. Lambin, Phys. Rev. B **57**, R15037 (1998).

[67] A.M. Rao, E. Ritcher, S. Bandow, B. Chase, P.C. Eklund, K.A. Williams, S. Fang, K.R. Subbaswamy, M. Menon, A. Thess, R. Smalley, G. Dresselhaus, M.S. Dresselhaus, Science **275** 187 (1997).

[68] M.A. Pimenta, A. Marucci, S.D.M. Brown, M.J. Matthews, A.M.Rao, P.C. Eklund, R.E. Smalley, G. Dresselhaus, M.S. Dresselhauss, J. Mater. Res. **13**, 2396 (1998); Phys. Rev. B **58**, R16016 (1998).

[69] P. Delaney, H.J. Choi, J. Ihm, S.G. Louie, M.L. Cohen, Nature **391**, 466 (1998).

[70] S.J. Tans, M.H. Devoret, H. Dai, A. Thess, R.E. Smalley, L.J. Geerligs, C. Dekker, Nature **386**, 474 (1997).

[71] S. Frank, P. Poncharal, Z.L. Wand, W.A. de Heer Science **280**, 1774 (1998).

[72] C.T. White and T.N. Todorov, *Nature* **393**, 240 (1998).

[73] L.C. Venema, J.W.C. Wildöer, T. Tuinstra, C. Dekker, A.G. Rinzler and R.E. Smalley, Appl. Phys. Lett. **71**, 2629 (1997). The cutting mechanism can be explained in terms of a mechanical instability induced by electrostatic stress due to the applied field (S.P. Apell, A. Rubio and C. Dekker, work in progress).

[74] H.-Y. Zhu, D.J. Klein, T.G. Schmalz, A. Rubio, N.H. March, J. Phys. Chem. Solids **59**, 417 (1997).

[75] M.F. Crommie, C.P. Lutz, D.M. Eigler, Science **262**, 218 (1993)

[76] M. Bockrath, D.H. Cobden, P.L. McEuen, N.G. Chopra, A. Zettl, A. Thess, R.E. Smalley, Science **275**, 1922 (1997).

[77] D. L. Carroll, P. Redlich, P. M. Ajayan, J. C. Charlier, X. Blase, A. De Vita, R. Car, Phys. Rev. Lett. **78**, 2811 (1997)

[78] X. Blase, A. Rubio, S.G. Louie and M.L. Cohen, Phys. Rev. B **51**, 6868 (1995)

[79] H. Dai, J.H. Hafner, A.G. Rinzler, D.T. Colbert, and R.E. Smalley, Nature **384**, 147 (1996).

[80] H. Dai, N. Franklin and J. Han, App. Phys. Lett. **73**, 1508 (1998)

[81] K. Suenaga, C. Colliex, N. Demoncy, A. Loiseau, H. Pascard and F. Willaime, Science **278**, 653 (1997).

[82] Y. Zhang, K. Suenaga, C. Colliex and S. Iijima, Science **281**, 973 (1998).